Chemical Geology 477 (2018) 151–160

Contents lists available at ScienceDirect

Chemical Geology

journal homepage: www.elsevier.com/locate/chemgeo

Mineral inclusion assemblage and detrital zircon provenance

Elizabeth A. Bell*, Patrick Boehnke[1,2], T. Mark Harrison, Matthew M. Wielicki[3]

Dept. of Earth, Planetary, and Space Sciences, University of California at Los Angeles, 595 Charles E. Young Dr. East/3806 Geology Building, Los Angeles, CA 90095, United States

ARTICLE INFO

Editor: Catherine Chauvel

Keywords:
Hadean
Archean
Zircon
Mineral inclusion
Detrital zircon

ABSTRACT

Mineral inclusions are common in magmatic zircon and a potentially rich source of petrologic information. Controls on the relative proportions of inclusion phases, specifically early-crystallizing minerals such as apatite and late-crystallizing phases such as quartz, K-feldspar, and muscovite, have not been systematically studied. For instance, apatite dominates many magmatic zircon inclusion suites, and selective replacement of apatite over other phases has been proposed as a mechanism for generating apatite-poor inclusion assemblages in detrital zircons. However, the extent to which apatite inclusion abundance is influenced by source rock composition has not been established. The preservation of characteristic minerals in granite series, such as differences in magnetite and ilmenite abundances due to varying redox, have also not been systematically explored as inclusion phases in zircon. We surveyed zircon inclusion assemblages in Phanerozoic granitoids of a range of compositions and found a broadly inverse relationship between the presence of apatite in the inclusion suite and whole-rock SiO_2 content. Selective loss of apatite is evident from deficits in apatite content among inclusions in contact with cracks in both detrital zircons and some granitoid zircons with independent evidence for fluid ingress (i.e., secondary phases filling open cracks). In cases where microstructural observations can identify primary inclusion assemblages (versus those impacted by fluid ingress), the relative occurrence of apatite can be used to broadly predict source rock SiO_2 content. There is little relationship between whole-rock chemistry and the abundance of late-crystallizing phases or the relative proportions of quartz, plagioclase, and alkali feldspar. The presence of ilmenite not in contact with cracks in the host zircon likely points to origins in ilmenite-series (i.e., reduced) magmas, but the presence of magnetite is less diagnostic. Using the apatite abundance metric, detrital Hadean zircons from Jack Hills (Western Australia), appear to derive from felsic rather than intermediate or mafic granitoids and detrital Eoarchean zircons from Nuvvuagittuq Supracrustal Belt (Quebec) may derive from intermediate to felsic granitoids. No Fe-Ti oxides have been identified in Nuvvuagittuq zircons, but rare ilmenite in Jack Hills zircons points to origins of at least some part of the population in ilmenite-series magmas.

1. Introduction

Detrital zircons provide a record of crustal evolution complementary to the crystalline rock record and indeed constitute the only known terrestrial materials surviving from the period before 4.03 Ga (Bowring and Williams, 1999; Mojzsis et al., 2014; Reimink et al., 2016; cf., O'Neil et al., 2008). For example, the geochemistry of 4.0 to 4.38 Ga detrital zircons from Jack Hills, Western Australia, has been interpreted to show the presence of a hydrosphere and relatively felsic crust as early as ca. 4.3 Ga (e.g., Mojzsis et al., 2001; Peck et al., 2001; Harrison et al., 2008). Mineral inclusions in detrital Hadean Jack Hills zircons have been used as a petrologic tracer of their source rocks. For example, Maas et al. (1992) inferred a broadly granitic source while Hopkins et al. (2008, 2010) used thermobarometry (in context of an S-type granite pseudosection) to estimate the geotherm in which Hadean Jack Hills magmas formed. The use of mineral inclusions to assess provenance, however, requires that the effects of secondary alteration of the inclusion suite be considered. Rasmussen et al. (2011) found that many monazite and xenotime inclusions in Jack Hills zircons have ages reflecting post-depositional metamorphism rather than formation in the original host magma. Further, they surveyed various granitoids and found that apatite dominates igneous zircon inclusion assemblages, whereas it comprises only a minor component of Jack Hills inclusions. They proposed that selective destruction of apatite inclusions had

* Corresponding author.
E-mail address: ebell21@ucla.edu (E.A. Bell).
[1] Now at Dept. of Geophysical Sciences, 5734 South Ellis Avenue, University of Chicago, Chicago, IL 60637.
[2] Now at Chicago Center for Cosmochemistry, Chicago, IL 60637.
[3] Now at Dept. of Geological Sciences, 2003 Bevill Building, University of Alabama, Tuscaloosa, AL 35487.

https://doi.org/10.1016/j.chemgeo.2017.12.024
Received 24 July 2017; Received in revised form 15 November 2017; Accepted 21 December 2017
Available online 24 December 2017

occurred due to exposure to surface- and groundwater during detrital zircon transport, deposition, and subsequent metamorphism (Rasmussen et al., 2011). Low apatite inclusion abundance among detrital zircons has also been found in North China Craton sandstone and quartzite by Nutman et al. (2014), who attributed it to the same process and proposed low apatite abundance as a marker for detrital zircon transport and sediment maturity.

However, factors determining the abundance of apatite and other phases in zircon-hosted mineral inclusion assemblages have not been systematically studied. In particular, the relative proportions of early (i.e., apatite) vs. late-crystallizing (i.e., quartz, K-feldspar, muscovite) inclusion abundance with source magma composition is uncertain. Several studies have reported varying apatite contents in magmatic zircon inclusion suites, and some studies have suggested that late-crystallizing phases will lead to inclusion assemblages which appear more felsic than the whole rock. For example, most Precambrian granitoids from the Rasmussen et al. (2011) survey have apatite-dominated inclusion assemblages, with the exception of a muscovite-biotite granite and a syenogranite. Nutman et al. (2014) report apatite dominance in orthogneiss zircons from the North China Craton whereas Jennings et al. (2011) found a preponderance of apatite inclusions in zircons from several intermediate to felsic granitoids from Dronning Maud Land, Antarctica. Darling et al. (2009) reported that zircons crystallized from different components of the Sudbury impact melt sheet contain varying pluralities of apatite and late inclusions. In addition, they reported that the proportions of quartz, plagioclase, and alkali feldspar in their Sudbury zircons were consistently shifted toward higher relative alkali feldspar and quartz contents relative to the whole rock, leading to an inclusion assemblage artificially resembling more felsic melts than the source rock. This effect is likely due to zircon's status as a late-crystallizing phase in most magmas, such that it is likely to capture a more felsic-looking assemblage than the whole rock. The magnitude of the shift is variable among the four lithologies Darling et al. (2009) studied, and the possibility of extracting provenance information from these phases remains unclear.

The likelihood of variable apatite abundance in magmatic zircon makes the significance of low apatite abundance in detrital zircons unclear and may plausibly reflect variable original apatite inclusion abundances, selective apatite destruction, or a combination of both. The significance of whole-rock composition for the abundance of late-crystallizing phases, or for the variable proportions of quartz, plagioclase, alkali feldspar in the inclusion assemblage is also uncertain. To address this issue, we present a survey of mineral inclusions in zircon from 24 granitoids with a range of compositions to investigate whether a) the occurrence of apatite in primary inclusion assemblages is a function of source rock composition; b) the occurrence of late-crystallizing phases (and the proportions of quartz and feldspars) is a function of source rock composition; and c) whether other phases such as redox-sensitive Fe-Ti oxides or sulfides can identify the magmatic sources of detrital zircons. We compare our results to inclusion assemblages of Hadean and Eoarchean detrital zircons from Jack Hills and the Nuvvuagittuq Supracrustal Belt, respectively, and search also for evidence of selective apatite destruction during fluid ingress into both detrital zircons and zircons from a highly weathered granitoid.

2. Methods

Zircons were extracted from 24 Phanerozoic granitoids ranging in composition from tonalite to granite and deriving from a variety of continental settings, including arcs and rifts (location and petrology details in electronic annex, document EA-4; whole-rock chemistry in Table EA-1). Whole-rock major and trace element chemistry were determined by X-ray fluorescence spectroscopy at Pomona College following double fusion of a 2:1 lithium tetraborate:rock powder mixture in graphite crucibles (method described by Poletti et al., 2016; analyses for most samples previously reported in Bell et al., 2017). Determination of magnetite vs. ilmenite series classification was based on examination of the opaque mineral fraction. We also obtained zircons from a highly weathered sample of the Baynton pluton (Lachlan Fold Belt, Victoria, Australia; Clemens et al., 2016), and an Eoarchean quartzite from the Nuvvuagittuq supracrustal belt containing abundant chromite as well as zircon with igneous Th/U and oscillatory zoning, interpreted by Cates and Mojzsis (2007) as a detrital sediment (NSB; unit Aqf; cf. Darling et al., 2013 for alternative interpretation of the unit's origins). Zircons were mounted in epoxy and polished with silicon carbide grinding paper to expose interiors. For granitoids with a high likelihood of zircon inheritance (as determined by zircon saturation thermometry; Boehnke et al., 2013), we searched for evidence of zircon inheritance using U-Pb geochronology using the CAMECA ims1270 ion microprobe at UCLA in order to identify and exclude inherited cores from the inclusion dataset. Conditions used were a ca. 15 nA primary O- beam focused to a ca. 20 μm diameter spot (see, e.g., Quidelleur et al., 1997 for analytical details). Geochronology data are found in the electronic annex, Table-EA-3.

Inclusions were identified by electron imaging and a combination of EDS and WDS X-ray spectroscopy on a Vega 3 XMU scanning electron microscope and a JEOL 8600 electron microprobe, respectively. Each inclusion was noted to be either isolated from or in contact with cracks in the host zircon (i.e., potential avenues for fluid ingress). Examples of these textures are shown in Figs. 1 and 2. Phases filling cracks (i.e., clearly secondary) were also noted. Inclusion occurrence was determined following the counting protocols of Bell (2016) and Bell et al. (2015), which considers each crack-isolated phase within a single zircon to be one occurrence of this phase. For example, a zircon containing three crack-isolated apatite inclusions and one isolated quartz inclusion will be considered to have contributed one apatite occurrence and one quartz occurrence to the overall count of crack-isolated inclusions. This approach does not allow for the estimation of the overall volume of the various included phases, but it is aimed at mitigating outsized effects from the hypothetical case of one zircon which happens to crystallize in a region of the melt which is unusually rich in a particular phase and could thus tilt the inclusion count toward an unrealistic view of the host magma if each individual inclusion were added to the total. Our results are reported as the percentage of crack-isolated phase occurrences of the specific phase. A parallel accounting of phase occurrences is kept for inclusions in contact with cracks and for phases filling cracks, respectively, for insights into alteration processes associated with cracks. The incidence of fluid flow along cracks was estimated by noting the presence of crack-filling (i.e., clearly secondary) phases. For most phases qualitative analysis by EDS sufficed for identification, while distinction between K-feldspar and muscovite, as well as pyrite and pyrrhotite, was made for some samples by WDS analysis. Mineral inclusion counts are listed in the electronic annex, Table EA-2.

3. Results

Among granitoid zircons, crack-isolated apatite was found in 1–75% of imaged zircons and comprised 3–79% of crack-isolated inclusions within zircons (Fig. 3a). Late-crystallizing phases (defined as quartz, alkali feldspar, and muscovite) comprised between 6% and 52% of crack-isolated inclusions in granitoid zircons (Fig. 4). Quartz, alkali feldspar, and plagioclase are present as isolated inclusions in almost all samples, with offsets toward higher alkali feldspar contents relative to their respective whole-rock compositions (Fig. 5), similar to the results of Darling et al. (2009) for zircons from the Sudbury impact crater. Similar offsets toward higher quartz among the inclusions are common but not universal, with a minority of suites showing similar or lower relative quartz than the whole rock composition would suggest (Fig. 5). Oxide and sulfide inclusions are rare, comprising in most cases < 5% of isolated inclusions but in one sample up to 13%. Oxides containing only Fe (likely magnetite) were identified in both ilmenite- and magnetite-

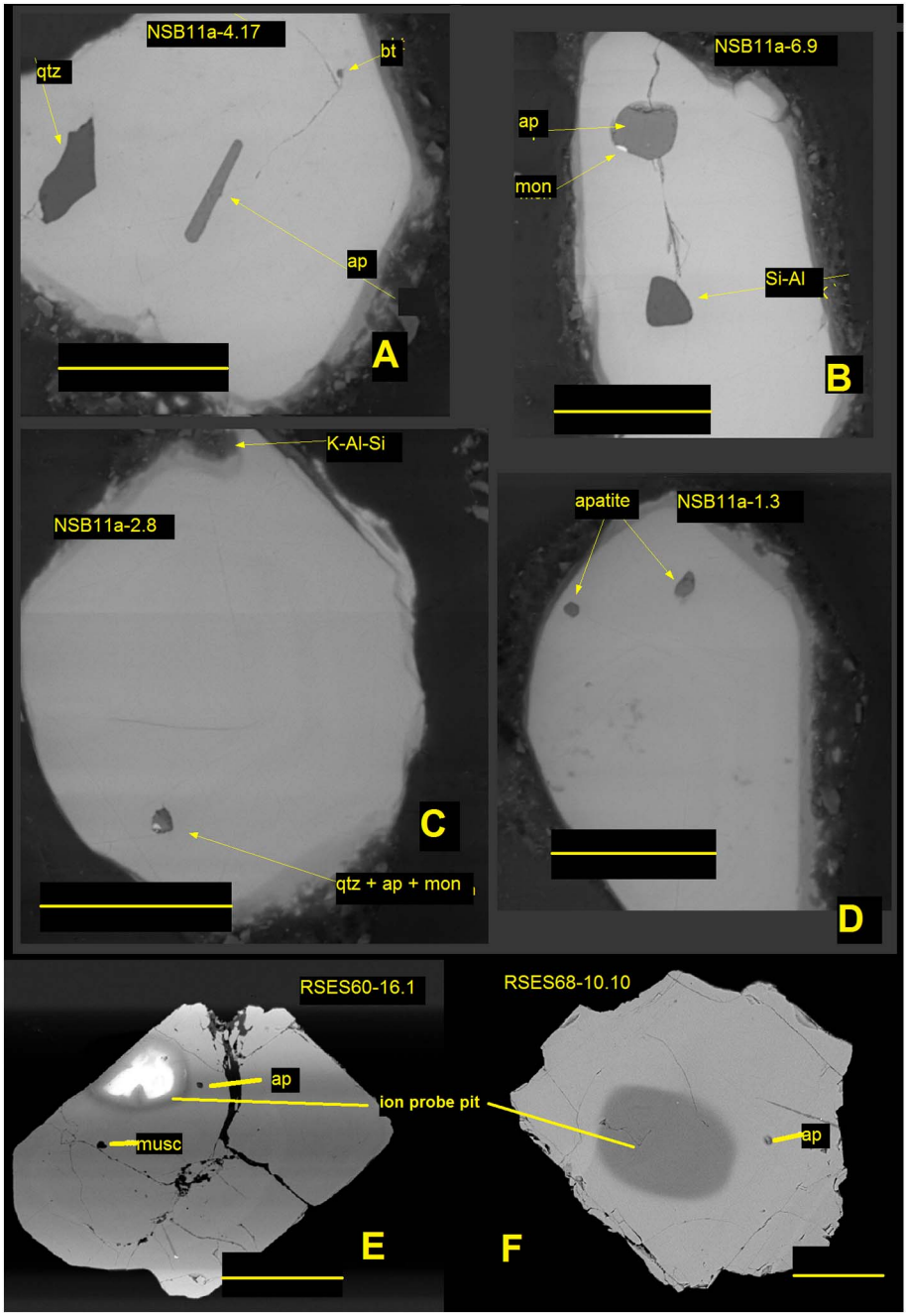

Fig. 1. Selected apatite inclusions in detrital zircons. A, C, D, E, F) Apatite inclusions of various sizes isolated from cracks in the host zircons. B) Apatite inclusion in contact with crack in host zircon. Apatite is found both as a single phase (as in A, D) and as part of multiphase inclusions (B, C). A–D are Nuvvuagittuq samples; E–F are Jack Hills samples imaged using a Leo 1430VP scanning electron microscope. Scale bars in each panel are 50 μm.

series zircons, while ilmenite is seen only among the ilmenite-series zircons (Fig. 6). Rutile is present in two suites. Pyrite is present as a rare, isolated inclusion phase in two ilmenite-series I-type suites (RG1 and RG5), while pyrrhotite inclusions are present in one ilmenite-series S-type suite (S1) both isolated from and in contact with cracks in the host zircon.

Crack-filling phases, including chlorite, biotite, Fe oxides, quartz, K-feldspar, and an Si-Al-Fe phase, were found in 0–17% of imaged zircons from each pluton. This point to variable degrees of secondary fluid flow affecting the zircons, and contrasting assemblages among inclusions isolated from and in contact with cracks suggest this has noticeable effects on the preserved inclusion cargo. Highly weathered Baynton granitoid, for instance, yielded 25 ± 6% (1σ based on counting statistics) apatite occurrence among crack-isolated inclusions, but only 1 ± 1% in contact with cracks (Fig. 3b). Apatite comprises 24 ± 4% of crack-isolated inclusion occurrences in magmatic (> 3.65 Ga; Cates et al., 2013) NSB zircons, but only 13 ± 3% of inclusions in contact with cracks or in metamorphic zircons at NSB (Fig. 3b). Crack-filling phases were found in 10% of Baynton zircons (including phases similar to those seen in other granitoid zircons as listed above) and 8% of NSB zircons (quartz, along with K-Al-Si and Al-Si phases). Among granitoid zircons, oxides containing only Fe (likely either magnetite or hematite) are more common in contact with cracks than in the isolated assemblage. In sample SpLb, which contains manganoan ilmenite in the rock matrix, the same ilmenite is present in contact with cracks but has not been identified within uncracked regions of the zircons. Isolated inclusions in Hadean JH zircons are 11% apatite, but no apatite is found in contact with cracks (Bell et al., 2015). One ilmenite and one Fe oxide phase are found in the isolated JH inclusion assemblage, and Fe oxides are a minor phase in the secondary assemblage filling cracks in the zircons (Bell et al., 2015).

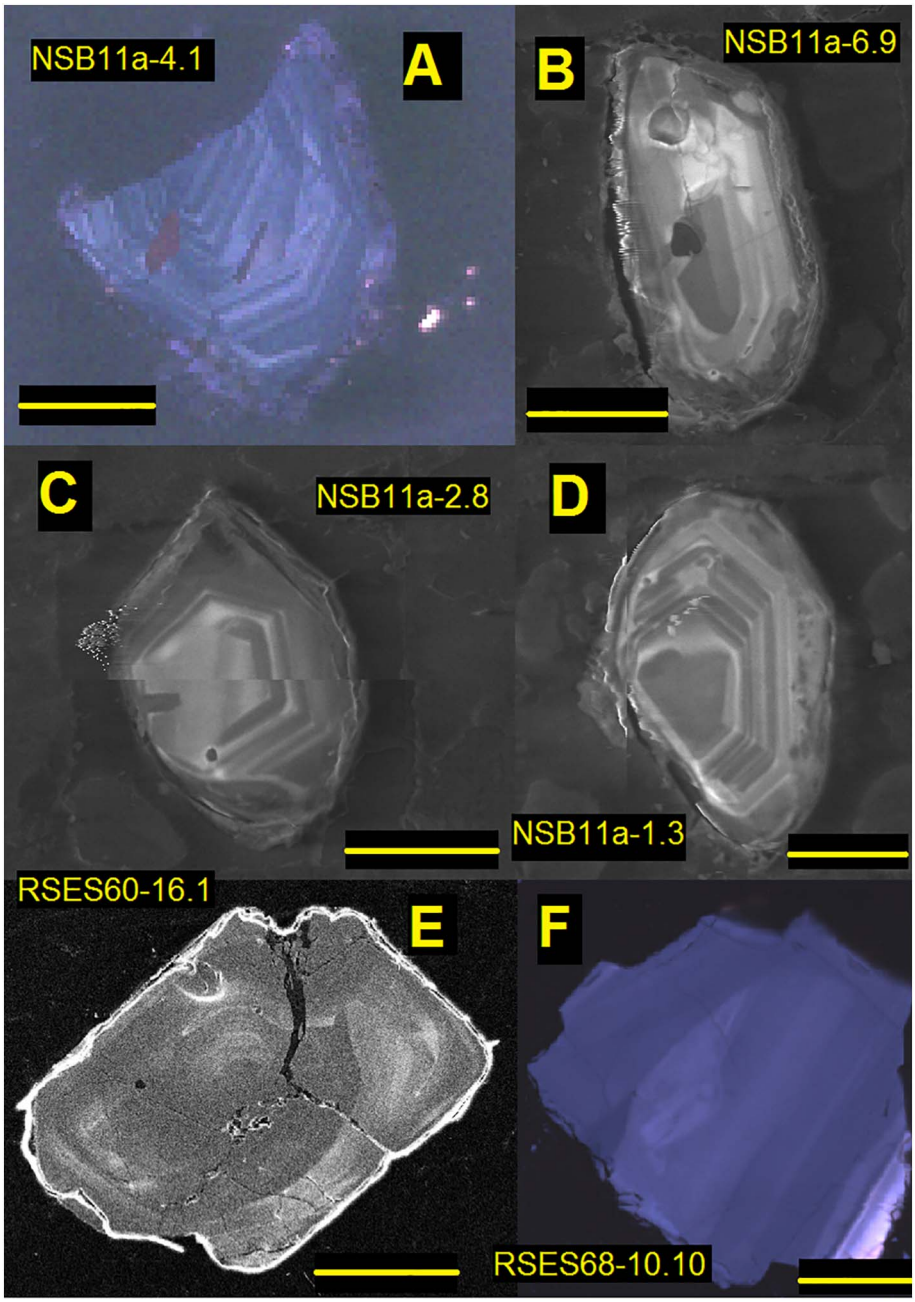

Fig. 2. Cathodoluminescence images of the detrital zircons shown in Fig. 1. E) was imaged using a Leo 1430VP scanning electron microscope. Scale bars in each panel are 50 μm.

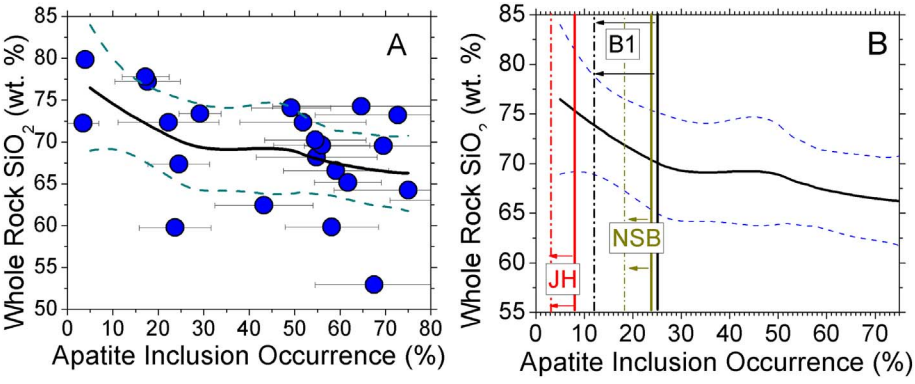

Fig. 3. Predicting whole-rock composition from apatite abundance. A) Whole-rock SiO_2 content vs. apatite inclusion occurrence in magmatic zircon. Solid curve: LOESS regression; dashed curves: 95% confidence interval. B) Predicted whole-rock SiO_2 for detrital Hadean zircons from Jack Hills (JH), detrital Archean zircons from Nuvvuagittuq Supracrustal Belt (NSB), and for zircons from a highly weathered granitoid (B1). Solid vertical lines: apatite abundance in isolated inclusion assemblages; dashed vertical lines: estimates for the same rock without accounting for selective apatite loss along cracks (i.e., using all inclusions).

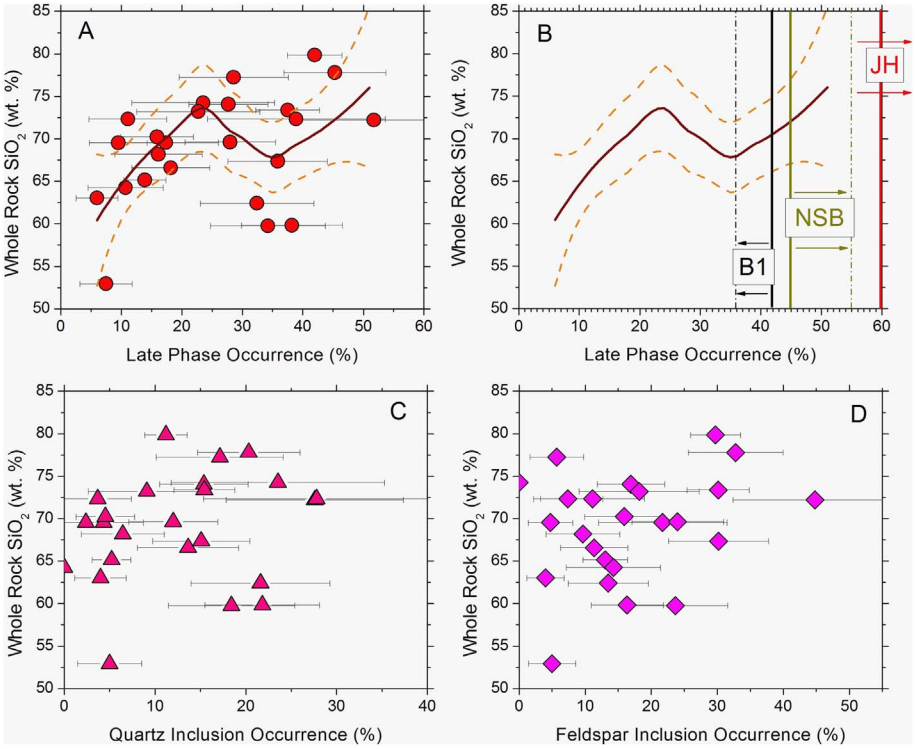

Fig. 4. Predictions for whole-rock composition from late phase (quartz, alkali feldspar, and muscovite) abundance are far more ambiguous than for apatite. A) Whole-rock SiO_2 content vs. late phase inclusion occurrence in magmatic zircon. Solid curve: LOESS regression; dashed curves: 95% confidence interval. B) Predicted whole-rock SiO_2 for detrital Hadean zircons from JH, detrital Archean zircons from NSB, and for zircons from a highly weathered granitoid (B1). Solid vertical lines: late phase abundance in isolated inclusion assemblages; dashed vertical lines: estimates using all inclusions. C) Whole rock SiO_2 vs. quartz abundance in the isolated inclusion assemblage. D) Whole rock SiO_2 vs. alkali feldspar abundance in the isolated inclusion assemblage.

4. Discussion

Large variations exist in the abundance and relative proportions of apatite, late-crystallizing phases, and redox-sensitive opaque phases in mineral inclusion assemblages of granitoid zircons. Apatite abundance and opaque phase occurrence vary with whole-rock chemistry, while the relationship between whole-rock chemistry and late-phase abundance or the relative proportions of quartz and various feldspars is much less clear.

4.1. Inclusion occurrence versus whole rock chemistry

Apatite inclusion abundance appears to be broadly indicative of whole-rock SiO_2, while late-crystallizing silicate phases have a weaker relationship with whole-rock chemistry. Fe-Ti oxide and sulfide inclusions, although minor phases in the inclusion assemblage, are helpful for discriminating origins in magnetite- vs. ilmenite-series granitoids.

4.1.1. Relationships with SiO_2

Fig. 3a shows a broadly inverse correlation between the frequency of apatite occurrence in the isolated inclusion suite and whole rock SiO_2. This general trend makes sense in terms of apatite saturation behavior – the solubility of apatite in silicate melts decreases systematically with decreasing temperature and increasing SiO_2 content (Harrison and Watson, 1984; Pichavant et al., 1992). When coupled with the potential for early apatite fractionation, Fig. 3a shows the expected trend. However, there is considerable scatter in the data (Fig. 3a). We first undertook a local regression (LOESS; Cleveland, 1979) to systemize the results in a form that can be used to estimate whole-rock SiO_2 from apatite inclusion occurrence (shown in Fig. 3 with 95% confidence interval bounds). LOESS is a non-parametric regression method which combines a moving window with a linear regression – that is, the closest data points to a given value of the independent variable are used to determine the local model fit. For example, at 11% apatite inclusion occurrence, the range of host SiO_2 contents predicted by the LOESS regression ranges from 69 to 79%. To assess the robustness of this calculation, we performed a bootstrap resampling of the original data with replacement (i.e., in each iteration, samples could be included more than once while others might be omitted entirely). This approach yields a 95% confidence interval for the Jack Hills (JH) source rock SiO_2 from 69.9 to 78.3%, indistinguishable from the LOESS regression prediction that used the

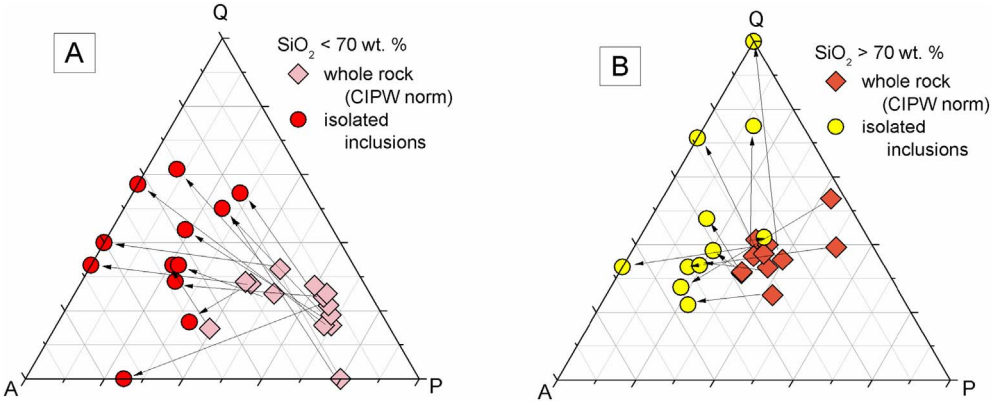

Fig. 5. Sampled granitoids in quartz (Q) – alkali feldspar (A) – plagioclase (P) space for both the whole-rock composition (relative mineralogy based on CIPW norm) and for isolated inclusion assemblages. Arrows connect whole rock compositions to inclusion assemblages. A) Sampled granitoids < 70 wt% SiO_2; B) sampled granitoids > 70 wt% SiO_2.

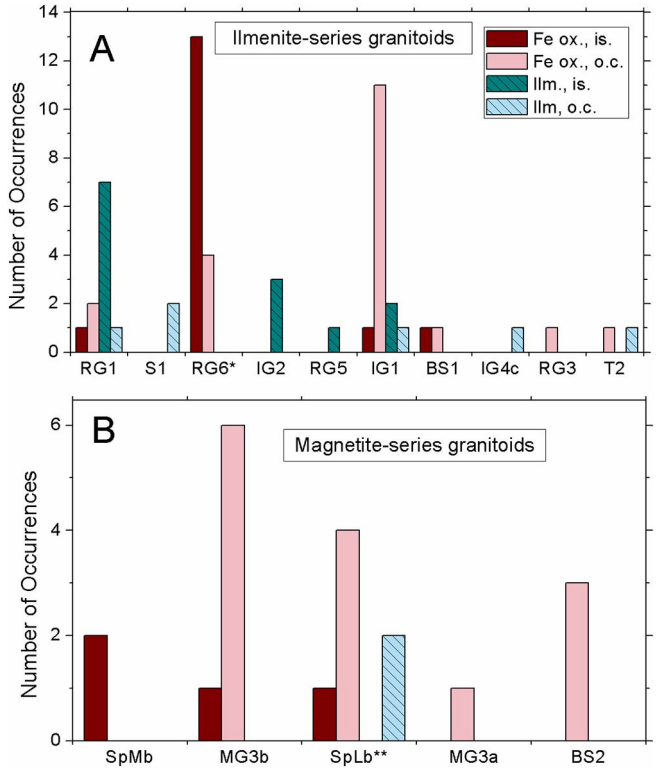

Fig. 6. Occurrence of Fe-Ti oxides relevant to whole rock redox state. A) Occurrence of Fe oxide and ilmenite in zircons from ilmenite-series (reduced) granitoids. B) Occurrence of these phases in magnetite-series (oxidized) granitoids. *RG6: is found within an ilmenite-series batholith but there is no clear matrix oxide component identified in thin section. **SpLb: is found within a magnetite-series batholith but the matrix is dominated by manganoan ilmenite of similar composition to that found along cracks in some of the zircons. "Fe ox": only Fe seen in the EDS spectrum; "Ilm": ilmenite; "is.": isolated from cracks; "o.c.": in contact with cracks.

original data, showing that outliers are not affecting the calculated values. While we might wish for a higher degree of correlation than we found (Fig. 3a), the relatively few tools available to those wishing to draw petrogenetic inferences from detrital zircons puts a premium on developing any potential proxy that could place bounds on their origin. We are confident that, within the stated error limits, this approach can discriminate between zircons formed in felsic melts (> 70% SiO_2) from those which formed in more silica deficient magmas.

By contrast, the abundance of inclusion phases which crystallize relatively late in the evolution of a magma – for which we use quartz, K-feldspar, and muscovite – show very little relationship with whole rock SiO_2, either as separate minerals or when taken together (Fig. 4). The relative QAP proportions of inclusion assemblages are almost all distinct from the whole rock composition (calculated from CIPW norms; Figs. 5, 7). Similarly to the results of Darling et al. (2009) for several lithologies from the Sudbury impact melt sheet, nearly all granitoids yield zircons with a higher ratio of alkali feldspar to plagioclase inclusions relative to the whole-rock (Fig. 7). The average volume alkali feldspar to alkali + plagioclase feldspar ratio (A/(A + P)) is 0.72 ± 0.18 (1σ) regardless of lithology. We did not observe A/(A + P) < 0.4 in our dataset. This leads to larger shifts in A/(A + P) for lower whole rock SiO_2 (Fig. 7e), but any particular A/(A + P) value is not mappable to a particular whole-rock composition. While most inclusion assemblages also have equal or higher quartz over total feldspar than the whole rock, some assemblages (mostly from the high-SiO_2 lithologies) show lower relative quartz (Fig. 7f). In short, there does not appear to be a clear way to reconstruct the whole-rock QAP or weight percent SiO_2 from either the observed alkali-feldspar/total feldspar or quartz/feldspar ratios of inclusions in zircon.

4.1.2. Relationships with f_{O2}

Granitoids vary widely in f_{O2}, with oxidized and reduced magmas typically containing distinct oxide species: oxidized magmas tend to be dominated by magnetite, and reduced magmas by ilmenite (Ishihara, 1977). Similar variations exist in sulfide species, with pyrrhotite dominating over pyrite in most Japanese and Sierra Nevadan ilmenite series granitoids and pyrite more common than pyrrhotite in the magnetite series (Ishihara and Sasaki, 1989). Our studied ilmenite series zircons contain minor amounts of oxide inclusions and rare sulfides. Ilmenite is the most common, although magnetite is also observed without ilmenite in two of the zircon suites (Fig. 6a). Pyrite inclusions are found in two I-type ilmenite-series zircons while pyrrhotite inclusions are found in one ilmenite-series S-type population. Oxides containing Fe exclusively are observed among isolated inclusions in magnetite-series zircons (Fig. 6b). They are found among the isolated assemblage for ilmenite-series zircons and also along cracks in both suites. Although a definitive mineralogical identification has not been made for these phases, the isolated phases are most likely to be magnetite based on the usual range of granitoid redox (e.g., Trail et al., 2015). Inclusions in contact with cracks, which may have been exposed to later fluid alteration, may be magnetite, hematite, or an Fe-oxyhydroxide alteration phase. Manganoan ilmenite was observed along cracks in sample SpLb, a leucogranite in which Mn-rich ilmenite is the dominant oxide in the rock matrix. (SpLb is placed in the magnetite-series category here since the rest of the batholith it was sampled from appears to be dominated by oxidized, magnetite-series granitoids). Overall, the presence of ilmenite in the isolated assemblage appears to be a good indicator for ilmenite-series origins, while the presence of magnetite is less diagnostic. The significance of sulfide inclusions may require further study, given their apparent rarity.

4.2. Likely controls on inclusion assemblages

4.2.1. Apatite saturation effects

As noted above, a likely control on the occurrence of apatite as an inclusion is the degree to which it saturates prior to or after the onset of zircon crystallization. Estimated apatite and zircon saturation temperatures calculated from whole-rock compositions can be inaccurate due to changing melt chemistry during fractional crystallization, and for zircon can underestimate the onset of saturation (e.g., ~80 °C for Himalayan granites; Harrison et al., 2007). Zircon solubility decreases with decreasing alkalis over network-forming melt constituents (M; Boehnke et al., 2013), effectively decreasing with progressive crystallization. Apatite solubility decreases with increasing SiO_2 content (Harrison and Watson, 1984) but dramatically increases once A/CNK (i.e., molar Al/(2 Ca + Na + K)) exceeds 1 (Pichavant et al., 1992). Fractional crystallization will cause felsic magmas to evolve toward lower M, higher A/CNK, and higher SiO_2. Although most granitoids in the study have A/CNK > 1 (average 1.05 ± 0.09), many may not have been peraluminous at the onset of zircon crystallization, since protracted crystallization of zircon is common in felsic magma chambers (e.g., Reid et al., 1997). We present estimates of the difference between calculated bulk rock apatite and zircon saturation temperatures accounting for the peraluminous nature of the present whole rocks (Fig. 8b), and also without this correction for A/CNK (Fig. 8c), which may better describe apatite saturation during much of the zircon crystallization history. Both estimates show a decrease in $\Delta T_{sat}^{ap\text{-}zir}$ with decreasing apatite inclusion occurrence – that is, apatite inclusions are less abundant in magmas with shorter temperature intervals over which apatite could crystallize before zircon saturated, suggesting that these respective saturation behaviors are a major factor controlling variations in apatite inclusion occurrence. Because the apatite-zircon saturation interval tends to decrease with increasingly SiO_2 – rich melts, this leads to the correlation between SiO_2 and apatite occurrence. One sample (granite BS1) lies off the correlations, likely due to its unusually low P/Zr ratio compared to its apatite occurrence rate (Fig. 8a) and SiO_2 (Fig.

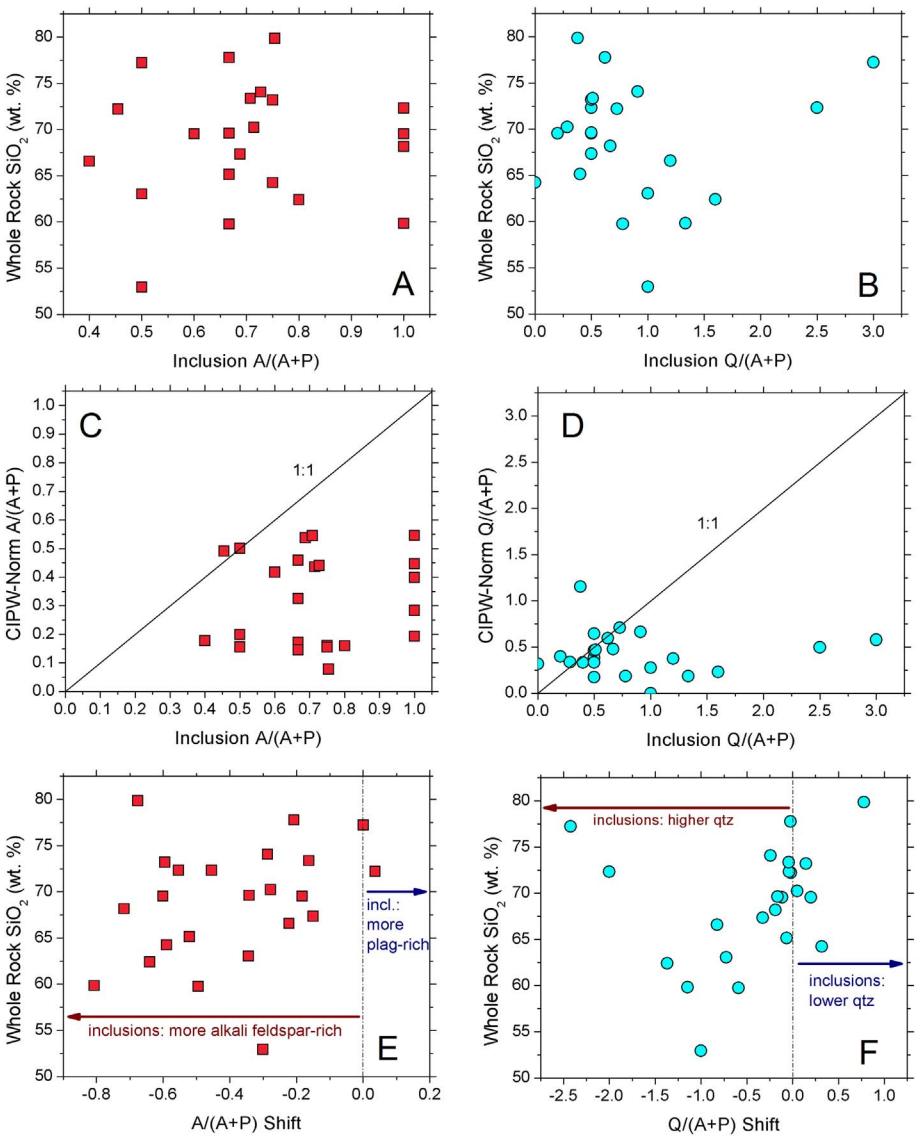

Fig. 7. Relationships of inclusion QAP and shifts in QAP composition between whole rock CIPW norm and isolated inclusion assemblage with granitoid composition. Shift is calculated as $X_{whole\ rock} - X_{inclusions}$. A) Whole-rock SiO_2 vs. the ratio of alkali feldspar over total feldspar A/(A + P) for inclusions; B) whole-rock SiO_2 vs. the ratio of quartz to total feldspar Q/(A + P) for inclusions. C) Whole-rock A/(A + P) vs. inclusion A/(A + P); D) whole-rock Q/(A + P) vs. inclusion Q/(A + P). E) Whole-rock SiO_2 vs. A/(A + P) shift; F) whole-rock SiO_2 vs. Q/(A + P) shift.

S-1 in EA-4).

4.2.2. Significance of QAP shifts

The nearly universal higher A/(A + P), and mostly higher Q/(A + P), among inclusion assemblages compared to source rock compositions means they appear to point to more highly evolved source magmas than the zircons are actually derived from (seen also by Darling et al., 2009; Jennings et al., 2011). This is likely due to zircon being a late-crystallizing phase in most granitoid magmas ("hot granites" of Miller et al., 2003), such that the phases available for inclusion in zircons are shifted toward higher Q/(A + P) and A/(A + P) than the whole rock. While it is possible that the large number of samples falling close to A/(A + P) = 0.8 (Figs. 5, 7) has greater significance for understanding the latest stages of melt evolution, this composition falls at much higher A/(A + P) than is generally expected for granite eutectic compositions (e.g., Wyllie, 1977). The amount of quartz at the eutectic varies with pressure and water content, although Q/(A + P) contents in the inclusion assemblages range higher than expected for eutectic compositions (Wyllie, 1977). The significance of these variations with respect to source magma character will require further targeted study.

4.3. Recognizing selective apatite loss

4.3.1. Loss of apatite along cracks

Cracks have clearly served as regions of fluid ingress in most zircon suites in this study, with crack-filling secondary phases found in both Archean quartzites and in all but one of the studied granitoids. In the case of the granitoid zircons, this likely reflects late-stage deuteric alteration of the pluton. Crack-filling phases in the JH zircons resemble the present host rock and probably result from metamorphic fluid flow during subsequent metamorphism (Bell et al., 2015). The detrital nature of the zircons, however, virtually guarantees their contact with surface- and groundwater during sedimentary transport and deposition.

Apatite is much less abundant in contact with cracks in the detrital zircons and zircons from the weathered granitoid, consistent with the Rasmussen et al. (2011) view that selective destruction of apatite inclusions occurs via surface- or groundwater ingress. Undetected, the selective destruction of apatite would bias estimations of whole-rock SiO_2 for detrital zircons toward more felsic compositions, as shown by the vertical dotted lines in Fig. 3b for detrital and weathered samples when crack-associated phases (with their apatite deficit) are also counted as part of the primary inclusion assemblage. Nine of the 24 studied granitoids also show a deficit of apatite inclusions along cracks in inclusion-hosting zircons (as noted in Fig. 8), and these granitoids are

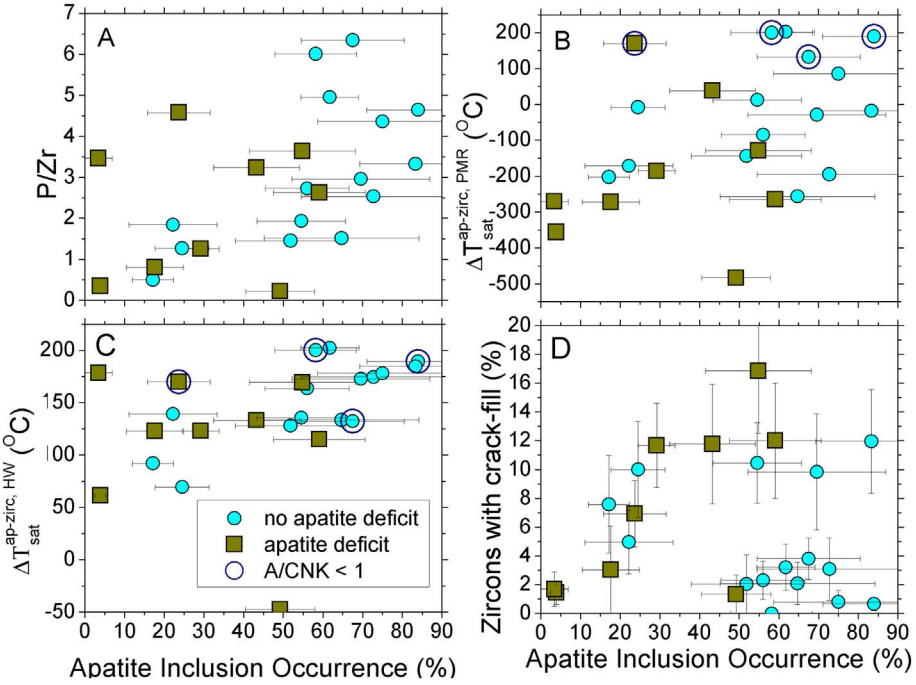

Fig. 8. Various aspects of apatite and zircon saturation behavior in the granitoid samples. All zircon saturation calculations use the model of Boehnke et al. (2013). Although only the inclusion suites isolated from cracks are considered in each panel, the granitoids are distinguished by whether or not zircons show an apatite deficit along cracks, in order to demonstrate that this alteration does not appear to extend to the isolated suite. A) Whole-rock P/Zr (ppm ratio) vs. apatite inclusions occurrence, B) estimated temperature intervals between onset of apatite and zircon saturation vs. apatite occurrence – using apatite saturation model of Pichavant et al. (1992); C) estimated saturation temperature intervals vs. apatite occurrence – using apatite saturation model of Harrison and Watson (1984); D) proportion of zircons containing secondary, crack-filling phases vs. apatite occurrence. There is a general correlation between the apatite inclusion abundance in zircon and the saturation temperatures for apatite and zircon. The gap between these temperatures also correlates with granite SiO_2 abundance, which probably accounts for the general trend for lower apatite inclusion abundance in zircon from more felsic magmas.

also more likely to show abundant secondary phases within cracks (Fig. 8d). Apatite was likely selectively destroyed by late-stage fluid flow in these cases, but this process appears to have been limited to inclusions along cracks since apatite occurrence in the overall primary suite is not correlated with the abundance of secondary phases (Fig. 8d) nor with the existence of an apatite deficit along cracks. Although in several of our granite suites, apatite inclusions are slightly more common in clearly magmatically zoned zircons, the offset between apatite abundance in clearly magmatically zoned regions versus the whole population of zircons is significant at the 1σ level in only one sample. The armoring of inclusions against fluid-related alteration away from cracks in their host zircon is likely widespread, also being suggested by the preservation of likely igneous plagioclase compositions away from cracks in a polymetamorphic Grenville orthogneiss (Bell, 2016), and preservation of readily-weathered apatite and feldspar only away from cracks in the JH zircons (Bell et al., 2015).

Since some volume of zircon has been destroyed during polishing in order to expose interior surfaces of our samples, the possibility remains that some of the studied inclusions which appear to be isolated from cracks were indeed in contact with cracks in the now-destroyed volume of zircon. This remains as a possibility for all studies of inclusions using polished samples, and for samples with apatite deficits this could lead to artificially low apparent primary apatite occurrences. Hidden cracks are likely not a significant factor for our zircons given the similar relationship of isolated apatite occurrence vs. SiO_2 and saturation temperature intervals for samples with and without crack-related apatite deficits (Fig. 8). This is further supported by the good match between evidence for fluid flow and occurrence of apatite deficits.

4.3.2. Apatite versus late phase abundance

Apatite abundance varies with late-phase abundance with a slope of approximately −0.4 (R^2 = 0.62; slope − 0.45 and R^2 = 0.72 using data from both our study and Rasmussen et al., 2011). This means that although apatite and late inclusion phases together make up the majority of inclusion phases, the proportions of other phases (e.g., plagioclase, biotite, hornblende, oxides) become greater at lower apatite abundance (Fig. 9). This relationship holds for isolated inclusions in granitoid zircon from the Phanerozoic (this study) and for inclusions reported by Rasmussen et al. (2011) from Precambrian granitoids. Highly silicic granitoids tend to yield zircons toward the low-apatite, high-late-phase end of the distribution, while lower-silica granitoids are more likely to be found toward the high-apatite, low-late-phase end of the distribution (Fig. 9b), although a fair amount of overlap leads to the same ambiguity at high apatite abundance as seen in Fig. 3.

Since magmatic zircon from a variety of tectonic settings and over a large portion of geologic history follow this relationship, it can be used to help identify selective apatite replacement in many cases. Replacement of apatite by quartz, K-feldspar, or muscovite (e.g., Rasmussen et al., 2011) would result in movement on a line of slope − 1 in the graph shown in Fig. 9, which could populate the region of the graph above the distribution of magmatic zircon. Replacement by phases other than quartz, K-feldspar, or muscovite would result in movement along a horizontal line and could populate the region below the magmatic zircon distribution. Detrital zircon suites falling within the low-apatite portion of the distribution could be the result of either sourcing from highly silicic granites or selective replacement of apatite by late phases without leaving textural evidence for the process. For instance, incorporating crack-intersecting inclusions in our detrital zircon suites shifts the samples to a lower-apatite position within the magmatic distribution. In the case that the cracks which served as pathways for fluid ingress are annealed by later metamorphism, the primary nature of the inclusion suite is ambiguous. Annealed cracks are evident in CL imaging of Jack Hills zircons (Bell et al., 2015), and inclusions armored in zircon from a Grenville orthogneiss appear to survive upper amphibolite to lower granulite facies metamorphism when there is no evidence for U-Pb disturbance (Bell, 2016), but further study is needed to determine the range of conditions under which primary inclusions are reliably preserved through later metamorphism and evidence for cracking and fluid flow is also reliably preserved.

4.4. Implications for detrital studies

Apatite inclusion chemistry shows promise as an indicator for aspects of detrital zircon source chemistry (e.g., Jennings et al., 2011; Bruand et al., 2016), and our results show that the presence of apatite in primary inclusion assemblages constitutes a parallel and complementary provenance record. Many zircons in this granitoid survey and those from Jack Hills (Bell et al., 2015; Hopkins et al., 2010), for

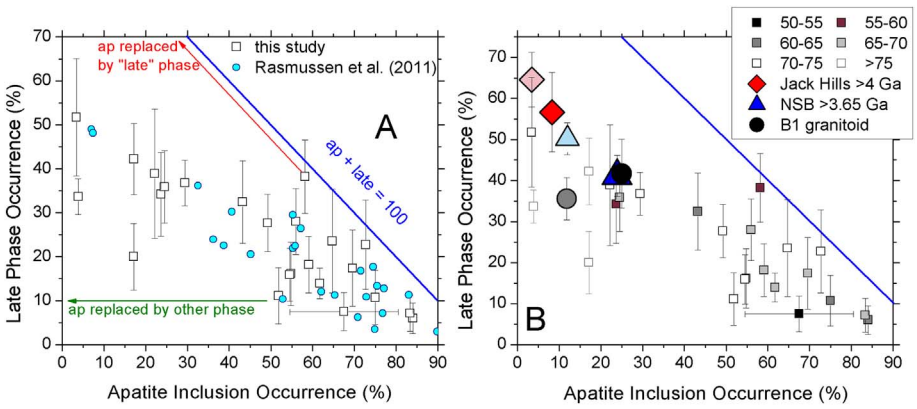

Fig. 9. Late phase inclusion occurrence vs. apatite inclusion occurrence for our studied granitoids and those from the literature. A) Granitoids from this study and the literature, with the trajectories of possible apatite replacement mechanisms illustrated. B) Granitoids from this study classified based on whole rock SiO_2 weight %, with isolated inclusion assemblages from detrital zircon suites (JH and NSB) and weathered granite (B1) shown. Detrital and weathered samples: dark symbol = isolated inclusion assemblage; muted symbol = assemblage in contact with cracks.

example, contain apatite inclusions too small for quantitative chemical analysis. In these cases, source rock information is still extractable from the inclusion record using apatite abundance. Additionally, the model of Bruand et al. (2016) involves estimating whole-rock Sr content from Sr in apatite, from which whole-rock SiO_2 can be estimated using separate trends for granitoids with Sr above and below 650 ppm. With apatite inclusion abundance as a separate estimate of whole-rock SiO_2, more certain assignment of whole-rock estimates to the appropriate trend may be possible in ambiguous cases. The JH zircons have low apatite inclusion occurrence, suggesting felsic origins. The LOESS prediction is less certain for more apatite-rich assemblages such as the NSB zircons, which may plausibly derive from felsic or more intermediate granitoids (Fig. 3). Mixing of zircons from multiple sources introduces complications for provenance schemes which use inclusion abundance rather than the chemistry of individual inclusions. However, the mixing of more felsic with more intermediate sources will likely result in an averaging of apatite inclusion abundance, such that this measure will still give overall compositional information – potentially distinguishing, for instance, a tonalite-dominated provenance from one of highly felsic origin such as that predicted for JH zircons. In this analysis JH zircons > 4.0 Ga were grouped together for the purposes of mineral inclusion counts, due to the lack of obvious changes in provenance from measures such as $\delta^{18}O$, trace elements, and inclusion suite during this period (Bell et al., 2015, 2016). NSB zircons with ages > 3.4 Ga were used, as they are likely derived from the 3.7–3.78 Ga concordant population after some Pb loss (Cates et al., 2013).

The occurrence of ilmenite inclusions in detrital zircon probably points to origins in ilmenite-series (reduced) granitoids, while magnetite inclusions are less diagnostic (Fig. 6). Although in this study sulfide inclusions were found only in ilmenite-series zircons, the presence of pyrite in some magnetite-series granites (e.g., Ishihara and Sasaki, 1989) may mean that pyrite inclusions specifically are not a universal indicator for reduced origins. More oxidized phases in contact with cracks may be alteration products following fluid ingress (Fig. 6). Hadean JH zircons so far studied have revealed one ilmenite and one magnetite inclusion isolated from cracks (Hopkins et al., 2010; Bell et al., 2015), suggesting origins of some > 4 Ga zircons from ilmenite-series granitoids. No oxide phases have been identified in the NSB zircons. Other markers for magma redox exist, including host zircon Ce/Ce^* (Trail et al., 2011). Given the overlap in calculated f_{O2} for I- vs. S-type zircons near the FMQ buffer (Trail et al., 2015), other markers will be useful in identifying provenance. Biotite Fe/Mg ratios are sensitive to magmatic f_{O2} (e.g., Abdel-Rahman, 1994; Ague and Brimhall, 1988; Burkhard, 1991). Given the good compositional match between matrix biotite and inclusions in zircon (Jennings et al., 2011; Bell et al., 2017), the distinct compositions of oxidized I-type and reduced S-type biotite can be used for provenance purposes. Distinction between oxidized and reduced I-type granites, or oxidized A-type granites, is more ambiguous (Bell et al., 2017) and oxide phases may be more helpful in assessing zircon provenance in these cases.

In this study we have only considered zircons from plutonic rocks, and it is unknown how inclusions in volcanic zircon may differ. Given the high volume ratio of plutonic to volcanic rocks in the continental crust, plutonic rocks are likely to dominate zircon sources except for some local areas. Future study of mineral inclusions in volcanic zircon may also be helpful in clarifying detrital zircon provenance in, for instance, sediments derived from volcanic arcs.

The apatite abundance method can only be applied to originally igneous zircon (e.g., distinguished by Th/U, etc.) and U-Pb age analysis should be used to distinguish age populations to be considered separately for apatite occurrence. In the case of texturally complex zircons with internal erosion surfaces or rim/core geometry, the rims and cores should be treated as separate age domains for inclusion-counting purposes. Zircons that appear from CL texture to be highly altered may not be amenable to apatite abundance provenance determinations, much as the same zircons may not preserve robust U-Pb ages for traditional zircon provenance analysis. As with all zircon-based provenance tools, this method is biased toward zircon-rich lithologies – i.e., intermediate to felsic rather than mafic sources.

5. Conclusions

Apatite abundance in igneous zircon mineral inclusion records is controlled both by selective destruction of apatite during later fluid alteration and by source magma composition, with primary inclusion suites showing a broad correlation between source rock SiO_2 and apatite abundance. Cataloguing of inclusions by relationship to microstructures in the host zircon which may be related to alteration or which may have allowed fluid ingress during sedimentary transport and deposition can help to identify the primary inclusion assemblage. Plotting detrital zircon suites in late phase vs. apatite occurrence space (as in Fig. 9) may also help to identify inclusion suites that have been affected by selective apatite loss. Other aspects of source rock composition are revealed by oxide inclusions: the presence of ilmenite inclusions suggests origins in ilmenite-series (reduced) granitoids, but magnetite inclusions may occur in either magnetite- (oxidized) or ilmenite-series zircons. Further studies of how efficiently zircon armors its inclusions against later weathering and metamorphism will be important for establishing the fidelity of such apparently primary inclusion records and whether alteration could still affect them over geologic time. These mineral inclusion-based provenance tools should be applicable for provenance reconstructions throughout the geologic record from the modern day to the Hadean, and may be used in a complementary fashion with provenance indicators based on host zircon age or mineral inclusion composition.

Acknowledgments

We thank Jonathan Harris for assistance with our XRF analyses, Rita Economos and Ming-Chang Liu for assistance with our SIMS analyses, and Andy Gleadow for his guidance in planning our sampling in the Lachlan Fold Belt. BSE images E and F in Fig. 1 and CL image E in Fig. 2 were taken by Michelle Hopkins. We are grateful to Roland Maas and an anonymous reviewer for comments which were very helpful in improving this manuscript. Nuvvuagittuq samples were collected during a field season led by Steve Mojzsis and supported by the Collaborative for Research in Origins (CRiO), which is funded by the John Templeton Foundation-FfAME Origins program. We are grateful for both Nicole Cates' and Steve Mojzsis' expertise at Nuvvuagittuq. The UCLA ion microprobe facility is partly supported by a grant from the Instrumentation and Facilities Program, Division of Earth Sciences, NSF (1339051). This work was further supported by CRiO, a Simons Collaboration on the Origins of Life Postdoctoral Fellowship to E.A.B. (293529), an NSF-EAR grant to T.M.H. (1551437), and the Chamberlin Postdoctoral Fellowship (Dept. of Geophysical Sciences, University of Chicago) to P.B.

Appendix A. Supplementary data

Supplementary data to this article can be found online at https://doi.org/10.1016/j.chemgeo.2017.12.024.

References

Abdel-Rahman, A.F.M., 1994. Nature of biotites from alkaline, calc-alkaline, and peraluminous magmas. J. Pet. 35, 525–541.
Ague, J.J., Brimhall, G.H., 1988. Regional variations in bulk chemistry, mineralogy, and the compositions of mafic and accessory minerals in the batholiths of California. GSA Bull. 100, 891–911.
Bell, E.A., 2016. Preservation of primary mineral inclusions and secondary mineralization in igneous zircon: a case study in orthogneiss from the Blue Ridge, Virginia. Contrib. Mineral. Petrol. 171, 1–15.
Bell, E.A., Boehnke, P., Hopkins, M.D., Harrison, T.M., 2015. Distinguishing primary and secondary inclusion assemblages in Jack Hills zircons. Lithos 234, 15–26.
Bell, E.A., Boehnke, P., Harrison, T.M., 2016. Recovering the primary geochemistry of Jack Hills zircons through quantitative estimates of chemical alteration. Geochim. Cosmochim. Acta 191, 187–202.
Bell, E.A., Boehnke, P., Harrison, T.M., 2017. Applications of biotite inclusion composition to zircon provenance analysis. Earth Planet. Sci. Lett. 473, 237–246.
Boehnke, P., Watson, E.B., Trail, D., Harrison, T.M., Schmitt, A.K., 2013. Zircon saturation re-revisited. Chem. Geol. 351, 324–334.
Bowring, S.A., Williams, I.S., 1999. Priscoan (4.00–4.03 Ga) orthogneisses from northwestern Canada. Contrib. Mineral. Petrol. 134, 3–16.
Bruand, E., Storey, C., Fowler, M., 2016. An apatite for progress: inclusions in zircon and titanite constrain petrogenesis and provenance. Geology 44, 91–94.
Burkhard, D.J., 1991. Temperature and redox path of biotite-bearing intrusives: a method of estimation applied to S-and I-type granites from Australia. Earth Planet. Sci. Lett. 104, 89–98.
Cates, N.L., Mojzsis, S.J., 2007. Pre-3750 Ma supracrustal rocks from the Nuvvuagittuq supracrustal belt, northern Québec. Earth Planet. Sci. Lett. 255, 9–21.
Cates, N.L., Ziegler, K., Schmitt, A.K., Mojzsis, S.J., 2013. Reduced, reused and recycled: detrital zircons define a maximum age for the Eoarchean (ca. 3750–3780 Ma) Nuvvuagittuq Supracrustal Belt, Québec (Canada). Earth Planet. Sci. Lett. 362, 283–293.
Clemens, J.D., Maas, R., Waight, T.E., Kunneke, L.K., 2016. Genesis of felsic plutonic magmas and their igneous enclaves: the Cobaw batholith of southeastern Australia. J. Geol. 124 (000–000).
Cleveland, W.S., 1979. Robust locally weighted regression and smoothing scatterplots. J. Am. Stat. Assoc. 74, 829–836.
Darling, J., Storey, C., Hawkesworth, C., 2009. Impact melt sheet zircons and their implications for the hadean crust. Geology 37, 927–930.
Darling, J.R., Moser, D.E., Heaman, L.M., Davis, W.J., O'Neil, J., Carlson, R., 2013. Eoarchean to Neoarchean evolution of the Nuvvuagittuq Supracrustal belt: new insights from U-Pb zircon geochronology. Am. J. Sci. 313, 844–876.
Harrison, T.M., Watson, E.B., 1984. The behavior of apatite during crustal anatexis: equilibrium and kinetic considerations. Geochim. Cosmochim. Acta 48, 1467–1477.
Harrison, T.M., Watson, E.B., Aikman, A.B., 2007. Temperature spectra of zircon crystallization in plutonic rocks. Geology 35, 635–638.
Harrison, T.M., Schmitt, A.K., McCulloch, M.T., Lovera, O.M., 2008. Early (≥ 4.5 Ga) formation of terrestrial crust: Lu-Hf, δ18O, and Ti thermometry results for hadean zircons. Earth Planet. Sci. Lett. 268, 476–486.
Hopkins, M., Harrison, T.M., Manning, C.E., 2008. Low heat flow inferred from > 4 Gyr zircons suggests Hadean plate boundary interactions. Nature 456, 493–496.
Hopkins, M., Harrison, T.M., Manning, C.E., 2010. Constraints on Hadean geodynamics from mineral inclusions in > 4 Ga zircons. Earth Planet. Sci. Lett. 298, 367–376.
Ishihara, S., 1977. The magnetite-series and ilmenite-series granitic rocks. Min. Geol. Tokyo 27, 293–305.
Ishihara, S., Sasaki, A., 1989. Sulfur isotopic ratios of the magnetite-series and ilmenite-series granitoids of the Sierra Nevada batholith—a reconnaissance study. Geology 17, 788–791.
Jennings, E.S., Marschall, H.R., Hawkesworth, C.J., Storey, C.D., 2011. Characterization of magma from inclusions in zircon: apatite and biotite work well, feldspar less so. Geology 39, 863–866.
Maas, R., Kinny, P.D., Williams, I.S., Froude, D.O., Compston, W., 1992. The Earth's oldest known crust: a geochronological and geochemical study of 3900–4200 Ma old detrital zircons from Mt. Narryer and Jack Hills, Western Australia. Geochim. Cosmochim. Acta 56, 1281–1300.
Miller, C.F., McDowell, S.M., Mapes, R.W., 2003. Hot and cold granites? Implications of zircon saturation temperatures and preservation of inheritance. Geology 31, 529–532.
Mojzsis, S.J., Harrison, T.M., Pidgeon, R.T., 2001. Oxygen-isotope evidence from ancient zircons for liquid water at the Earth's surface 4300 Myr ago. Nature 409, 178–181.
Mojzsis, S.J., Cates, N.L., Caro, G., Trail, D., Abramov, O., Guitreau, M., Blichert-Toft, J., Hopkins, M.D., Bleeker, W., 2014. Component geochronology in the polyphase ca. 3920 Ma Acasta Gneiss. Geochim. Cosmochim. Acta 133, 68–96.
Nutman, A.P., Maciejowski, R., Wan, Y., 2014. Protoliths of enigmatic Archaean gneisses established from zircon inclusion studies: case study of the Caozhuang quartzite, E. Hebei, China. Geosci. Front. 5, 445–455.
O'Neil, J., Carlson, R.W., Francis, D., Stevenson, R.K., 2008. Neodymium-142 evidence for hadean mafic crust. Science 321, 1828–1831.
Peck, W.H., Valley, J.W., Wilde, S.A., Graham, C.M., 2001. Oxygen isotope ratios and rare earth elements in 3.3–4.4 Ga zircons: ion microprobe evidence for high $\delta^{18}O$ continental crust and oceans in the early Archean. Geochim. Cosmochim. Acta 65, 4215–4299.
Pichavant, M., Montel, J.M., Richard, L.R., 1992. Apatite solubility in peraluminous liquids: experimental data and an extension of the Harrison-Watson model. Geochim. Cosmochim. Acta 56, 3855–3861.
Poletti, J.E., Cottle, J.M., Hagen-Peter, G.A., Lackey, J.S., 2016. Petrochronological constraints on the origin of the mountain pass ultrapotassic and carbonatite intrusive suite, California. J. Pet. 57, 1555–1598.
Quidelleur, X., Grove, M., Lovera, O.M., Harrison, T.M., Yin, A., Ryerson, F.J., 1997. The thermal evolution and slip history of the Renbu Zedong thrust, southeastern Tibet. J. Geophys. Res. 102, 2659–2679.
Rasmussen, B., Fletcher, I.R., Muhling, J.R., Gregory, C.J., Wilde, S.A., 2011. Metamorphic replacement of mineral inclusions in detrital zircon from Jack Hills, Australia: implications for the hadean earth. Geology 39, 1143–1146.
Reid, M.R., Coath, C.D., Harrison, T.M., McKeegan, K.D., 1997. Prolonged residence times for the youngest rhyolites associated with Long Valley Caldera: 230Th—238U ion microprobe dating of young zircons. Earth Planet. Sci. Lett. 150, 27–39.
Reimink, J.R., Chacko, T., Stern, R.A., Heaman, L.M., 2016. The birth of a cratonic nucleus: lithogeochemical evolution of the 4.02–2.94 Ga Acasta Gneiss complex. Precambrian Res. 281, 453–472.
Trail, D., Watson, E.B., Tailby, N.D., 2011. The oxidation state of Hadean magmas and implications for early Earth's atmosphere. Nature 480, 79–82.
Trail, D., Tailby, N.D., Sochko, M., Ackerson, M.R., 2015. Possible biosphere-lithosphere interactions preserved in igneous zircon and implications for Hadean Earth. Astrobiology 15, 575–586.
Wyllie, P.J., 1977. Crustal anatexis: an experimental review. Tectonophysics 43, 41–71.